Chemistry & Biology
Article

Glucocorticoid Compounds Modify Smoothened Localization and Hedgehog Pathway Activity

Yu Wang,[1,2,3,7] Lance Davidow,[1,4] Anthony C. Arvanites,[1,4] Joel Blanchard,[1,4,8] Kelvin Lam,[1,4,9] Ke Xu,[1,4] Vatsal Oza,[1,4] Jin Woo Yoo,[5] Jessica M.Y. Ng,[6] Tom Curran,[6] Lee L. Rubin,[1,4,*] and Andrew P. McMahon[1,2,4,10,*]
[1]Department of Stem Cell and Regenerative Biology
[2]Department of Molecular and Cellular Biology
[3]Department of Chemistry and Chemical Biology
[4]Harvard Stem Cell Institute
[5]Harvard College
Harvard University, Cambridge, MA 02138, USA
[6]Children's Hospital of Philadelphia, Philadelphia, PA 19104, USA
[7]Present address: The Morgridge Institute for Research, Madison, WI 53715, USA
[8]Present address: The Scripps Research Institute, La Jolla, CA 92037, USA
[9]Present address: Blue Sky Biotech, Inc., Worcester, MA 01605, USA
[10]Present address: Department of Stem Cells and Regenerative Medicine, University of Southern California, 1425 San Pablo Street, Los Angeles, CA 90089, USA
*Correspondence: lee_rubin@harvard.edu (L.L.R.), amcmahon@mcb.harvard.edu (A.P.M.)
http://dx.doi.org/10.1016/j.chembiol.2012.06.012

SUMMARY

The Hedgehog signaling pathway is linked to a variety of diseases, notably a range of cancers. The first generation of drug screens identified Smoothened (Smo), a membrane protein essential for signaling, as an attractive drug target. Smo localizes to the primary cilium upon pathway activation, and this transition is critical for the response to Hedgehog ligands. In a high content screen directly monitoring Smo distribution in Hedgehog-responsive cells, we identified different glucocorticoids as specific modulators of Smo ciliary accumulation. One class promoted Smo accumulation, conferring cellular hypersensitivity to Hedgehog stimulation. In contrast, a second class inhibited Smo ciliary localization and signaling activity by both wild-type Smo, and mutant forms of Smo, SmoM2, and SmoD473H, that are refractory to previously identified Smo antagonists. These findings point to the potential for developing glucocorticoid-based pharmacological modulation of Smo signaling to treat mutated drug-resistant forms of Smo, an emerging problem in long-term cancer therapy. They also raise a concern about potential crosstalk of glucocorticoid drugs in the Hedgehog pathway, if therapeutic administration exceeds levels associated with on-target transcriptional mechanisms of glucocorticoid action.

INTRODUCTION

The Hedgehog (Hh) pathway is one of the central pathways of animal development, and deregulated pathway activity underlies a multitude of diseases, notably a variety of cancers (Rubin and de Sauvage, 2006). Activating mutations in Hh pathway components are cell intrinsic causal factors in cancers linked to Gorlin syndrome, medulloblastoma (MB), basal cell carcinoma (BCC), and rhabdomyosarcoma. In addition, paracrine Hh signaling-based modulation of the tumor microenvironment is thought to play a wider role in the support of a number of other malignancies including those of the breast, lung, liver, stomach, pancreas, prostate, and colon (Yauch et al., 2008). Hh signaling is also linked to medically beneficial actions such as the promotion of stem/progenitor cell proliferation that may enable regenerative therapies. Considerable clinical interest has developed about the mechanisms of Hh pathway action and the identification of drugs that can modulate pathway activity.

Smoothened (Smo), a seven-pass transmembrane protein, has emerged as a predominant target in screens for small-molecule pathway modulators. Smo is essential for all Hh signaling (Zhang et al., 2001). All 7 drugs in clinical trials for Hh targeted cancer therapy act directly on Smo to inhibit Hh signaling (Tremblay et al., 2010). Among these, GDC0449 (also known as RG3616 or Vismodegib), was recently approved by the US Food and Drug Administration (FDA) for indication of advanced BCC (Allison, 2012). On the other hand, it was reported that administration of at least two clinical Smo antagonists (GDC0449 and LDE225) resulted in cancer relapse in human and/or mouse in part due to emergence of drug resistant mutations of Smo, which highlighted an unmet medical need for next generation Smo antagonists that can circumvent such mutations (Buonamici et al., 2010; Yauch et al., 2009). Smo regulation is quite unusual. Hh binding to its receptor Patched-1 (Ptch1) counters Ptch1 mediated inhibition of Smo, enabling Smo-dependent activation of a Gli-based transcriptional response (Rohatgi et al., 2007). These events correlate with, and are critically linked to, the primary cilium (PC), a tubulin-based cell extension present on most vertebrate cells (Goetz and Anderson, 2010). After binding Hh, Ptch1 moves from the PC while Smo accumulates on the ciliary axoneme.

Though the mechanistic details are unclear, Smo action at the PC is essential for pathway activation (Han et al., 2009; Wong et al., 2009), and this cellular translocation presents an opportunity for novel drug development.

Here, we report on a high content screen (HCS) to identify small molecules that modulate Smo accumulation at the PC. Most strikingly, we identified a large number of glucocorticoids (GCs), several of which are in clinical use, that induce this activity. Surprisingly, these compounds fail to trigger robust pathway activation; instead, they sensitize cells to Hh ligand input and impair pathway inhibition by coadministered pharmacological antagonists of Smo signaling. In contrast, another steroid, budesonide, inhibits Smo ciliary translocation and Hh signaling, synergizing with GDC0449, a Smo antagonist under clinical evaluation. Importantly, budesonide acts similarly on wild-type Smo, and mutant forms refractory to other Smo antagonists, SmoM2 and SmoD473H (Xie et al., 1998; Yauch et al., 2009). These findings have important ramifications for the design of new therapeutic approaches to treat cancers whose growth can be modulated by Smo activation, and potential implications for off-target crosstalk of glucocorticoid drugs in the Hedgehog signaling pathway.

RESULTS

Development of a HCS to Identify Agonists of Smo Ciliary Accumulation

To gain a more comprehensive view of the Hh pathway at early stages of drug development, we developed and validated a HCS method based directly on Smo translocation to the PC (Wang et al., 2012). Herein, we report our findings while using the method to identify agonists of Smo ciliary accumulation. An enhanced green fluorescent protein (EGFP)-tagged form of human Smo was introduced into Hh-responsive NIH 3T3 cells (Wang et al., 2009) (Figure S1A available online) to generate a clonal cell line in which Hh-dependent accumulation of Smo::EGFP in the PC mirrored movement of endogenous Smo (Wang et al., 2009). An Inversin(Ivs)::tagRFPT expression cassette provided a constitutive, independent PC marker (Watanabe et al., 2003).

Custom algorithms were developed to perform quantitative multiparametric image analyses (Wang et al., 2012). Robust dose-dependent responses were observed upon treatment with several known small molecule modulators of Smo: the agonist SAG and the antagonist cyclopamine (Cyc), both of which directly bind Smo, and forskolin (FKL), whose stimulatory action on protein kinase A inhibits Smo signaling (Figures S1A–S1F). Despite the fact that Cyc and SAG physically interact with Smo in a competitive fashion suggesting a common binding mechanism, and that both induce ciliary accumulation, Cyc-bound Smo is inactive. Thus, accumulation within the primary cilium appears to be essential but not sufficient for downstream activation of the Hh pathway. In contrast, FKL likely induce Smo ciliary accumulation indirectly potentially by accelerating anterograde intraflagellar transport (Besschetnova et al., 2010). A better understanding awaits a clearer picture of the cellular trafficking processes. As a demonstration of the assay's ability to detect local changes within the PC, elongation of the PC on FKL treatment was detected as an expanded Ivs+ domain (last panel in Figure S1F), consistent with a recent report (Besschetnova et al., 2010).

Screening Results

We conducted a screen with a library consisting of 5,672 compounds with annotated activities, including FDA-approved drugs and drug candidates in preclinical or clinical development. Representative examples of plates including small-molecule control wells are shown for the analysis (Figure S1G). Z-prime scores (Zhang et al., 1999) consistently >0.4 indicate a reasonable reliability of the primary screen.

Approximately 60 compounds in 15 distinct chemical classes were confirmed to induce Smo accumulation at the PC, after rigorous assessment of the dose-response curves for primary hits. As expected, these comprised both pathway agonists and antagonists. For example, LY 294002, an inhibitor of phosphatidylinositol 3-kinase (PI3K) (Vlahos et al., 1994), induces Smo ciliary accumulation, but inhibits Hh signaling (Figures S1H–S1K). The PI3K pathway is important in a variety of cancer types and may intersect with the Hh pathway in tumorigenesis (Hambardzumyan et al., 2008). In combination treatment, a PI3K inhibitor and a Smo antagonist delayed the onset of drug resistance in a mouse model of medulloblastoma (Buonamici et al., 2010; Dijkgraaf et al., 2011). PI3K action has also been linked to the regulation of Gli proteins through the Akt pathway (Riobó et al., 2006). These data suggest that PI3K may act at multiple levels in Hh signaling.

Strikingly, the most predominant chemical class identified comprised naturally occurring and synthetic GCs, several of which are widely used as antiinflammatory agents in the clinic (Figures 1A and 1B; Figure S1L) (Sommer and Ray, 2008). Interestingly, a recent screen examining β-arrestin aggregation identified an overlap with a subset of these compounds, lending additional support to a GC intersection in Smo-directed Hedgehog signaling, but also raising the possibility of alternative mechanisms (Wang et al., 2010). Structure-activity relationship (SAR) analysis suggests that fluorine at position 9, a ketal at positions 16 and 17, and protonation at position 11 significantly enhance the potency of this class of compounds in directing Smo accumulation to the PC (Figure 1C).

GCs Accumulate Smo in the PC without Activating the Hh Pathway

To investigate in more detail the consequences of GC-induced Smo accumulation in the PC, and to obtain mechanistic insights into GC action in the Hh pathway, we first chose one compound in clinical use, fluocinolone acetonide (FA). FA displays an EC_{50} of around 5 μM for accumulation of Smo in the PC; in addition, no obvious cytotoxic effects are observed in vitro at much higher doses (up to 200 μM; Figures 1B and 1D; Figure S1M). Localization of an inversin-based PC reporter and other PC markers including Arl13b, acetylated tubulin, and detyrosinated α-tubulin (glu-tub) were unaltered in response to FA (Figure 1D; Figures S1M and S1N) (Caspary et al., 2007; Schrøder et al., 2007; Watanabe et al., 2003). Further, no change was detected in the activity of a Wnt-signaling reporter in response to FA concentrations that modify Smo distribution (Figure S1O). Together, these data suggest that FA's effects in this assay are specific to the Hh pathway.

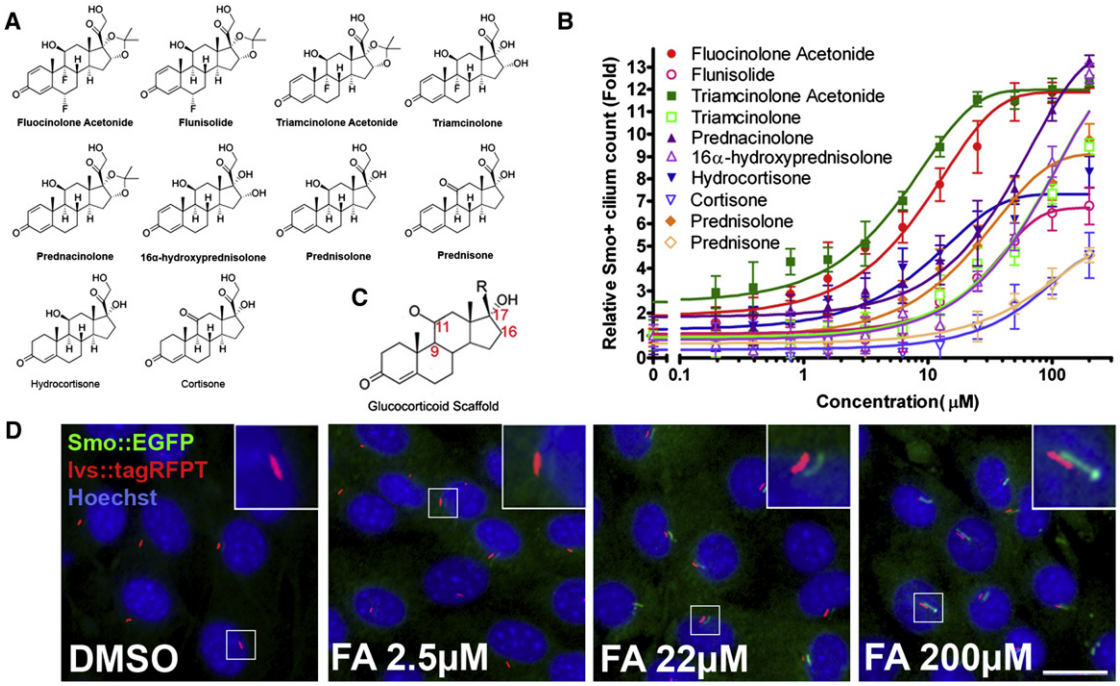

Figure 1. Glucocorticoids Induce Smo Accumulation at the Primary Cilium

(A) Structures of ten representative naturally occurring and synthetic GCs (names in bold).

(B) Related dose-response curves for accumulation of Smo in the PC using the subset of GCs indicated in (A). The mean (± SD) was calculated for four replicates analyzing several hundred cells in each sample.

(C) Key positions correlating with Smo accumulation activity in the GC scaffold are highlighted in red.

(D) Representative images of dose-dependent accumulation of Smo at the PC in response to stimulation by a synthetic GC, fluocinolone acetonide (FA). Scale bar: 10 μm.

See also Figures S1 and S4.

The accumulation of Smo in the PC is thought to be essential for transcriptional activation of the Hh pathway (Kim et al., 2009; Rohatgi et al., 2007). However, we observed a marked disparity between FA-induced Smo accumulation in the PC and Hh pathway activation in transcription reporter assays. At low levels of FA that effectively promote Smo accumulation in the PC (10 μM), no pathway activation was observed. Higher concentrations (>50 μM) invoked a weak transcriptional response measurable in a Gli-luciferase reporter assay (4-fold versus 25-fold for 1 μM of the Smo agonist SAG in the same assay [data not shown]), and on quantitative reverse transcription (qRT)-PCR measurement of Hedgehog target gene expression (*Ptch1* and *Gli1*; Figures 2A and 2B). The EC_{50} for weak transcriptional activation (>50 μM) was 10-fold higher than that of FA-induced accumulation of Smo within the PC.

FA Induces Hypersensitivity to Hh Pathway Stimulation

The effects of FA resemble overexpression of Smo in that constitutive accumulation of wild-type Smo within the PC only results in weak pathway activation (Figure S2A). Ciliary accumulation of Smo sensitizes cells to subsequent Sonic hedgehog (Shh) ligand input, raising the possibility that FA-driven Smo accumulation may sensitize Hh-responsive cells. Indeed, costimulation of cells with 10 μM FA results in a dose-dependent enhancement of a Shh-induced transcriptional response (Figures 2C and 2D). Furthermore, this effect was measurable after prolonged withdrawal of FA; cells treated for 24 hr with FA followed by compound withdrawal prior to Shh addition showed a higher induction of pathway activity than DMSO-treated controls (Figures 2E and 2F). The EC_{50} of a FA-induced response to priming is approximately 4 μM, in good agreement with the dose required for efficient accumulation of Smo in the PC (Figure 1B). Smo turnover in the PC is relatively slow after Shh-invoked pathway activation (Wang et al., 2009), or compound withdrawal (Figures S2B and S2C), providing a potential explanation for a FA-induced pathway priming effect. FA treatment showed no effect on Wnt pathway activity (Figure S1O), consistent with Hh pathway specificity.

FA May Regulate Smo by Direct Binding

To determine whether FA interacts with Smo, we performed a competition assay with Bodipy-Cyc. Cyc binds Smo directly (Chen et al., 2002a) and its fluorescent analog, Bodipy-Cyc, shows strong Smo-dependent fluorescence within cells overproducing Smo (identified by coexpression of a nuclear localized tagRFP-T; Figures 2G and 2H). An oncogenic mutation within the seventh transmembrane domain (SmoM2, also named SmoA1; Figures 2H and 2I) (Chen et al., 2002a), and a recently described drug resistance mutation within the sixth transmembrane domain (SMOD473H) significantly impair Cyc binding to Smo, suggesting that these are critical sites for chemical interaction (Yauch et al., 2009).

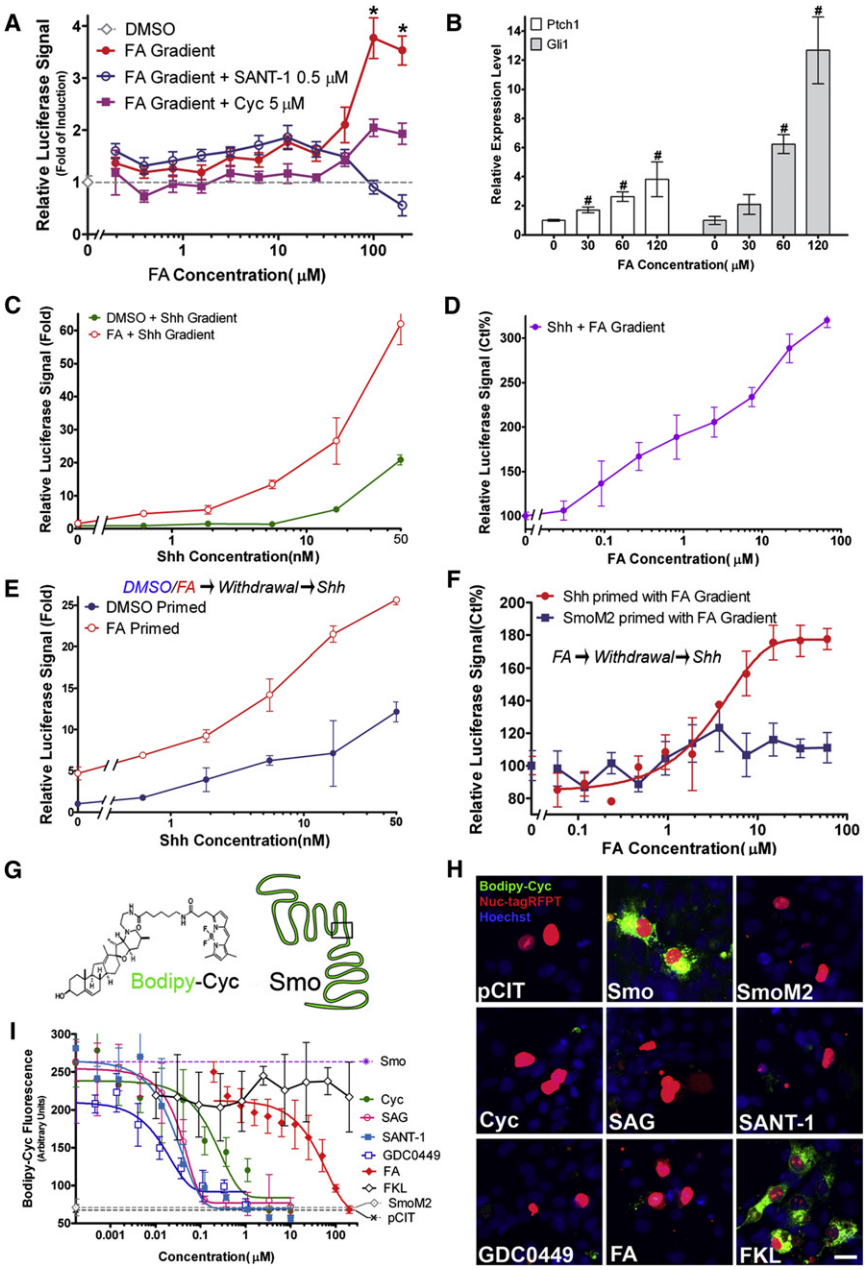

Figure 2. FA Sensitizes Cells to Hh Stimulation and Competes with Cyc Binding to Smo

(A) Modest but significant activation of the Hh pathway at high doses of FA, measured by a Gli-responsive luciferase reporter activity in NIH/3T3 cells. FA action is blocked by Smo antagonists SANT-1 and Cyc. *$p < 0.0001$ (t test), comparing with DMSO, FA+SANT-1, or FA+Cyc.

(B) FA upregulates the expression of Hh target genes *Ptch1* and *Gli1* in NIH/3T3 cells. #$p < 0.02$ (t test).

(C and D) Measurement of Hh pathway activity in cells treated simultaneously with a fixed concentration of FA and different concentrations of Shh ligand (C), or with a fixed concentration of Shh ligand, and different concentrations of FA (D). Treatment with Shh ligand and DMSO were used for comparison.

(E) Measurement of Hh pathway activity after stimulation with various concentrations of Shh ligand following priming treatments with 10 μM FA (red curve). DMSO prime treatments (blue curve) were used for comparison.

(F) Measurement of Hh pathway activity after stimulation with a fixed dose of Shh ligand following priming treatments with different concentrations of FA (red curve) or when pathway activity was stimulated by expressing a constitutively active SmoM2 variant (blue curve). All Gli-luciferase assay samples were replicated four times. The qRT-PCR in (B) was performed in triplicate. Data represent mean (± SD).

(G) Schematics showing the structures of Bodipy-Cyc and Smo. Critical sites in the sixth and seventh transmembrane domains of Smo, that are likely important for direct interactions are highlighted by a rectangle.

(H) Representative merged images from Bodipy-Cyc competition assays. Transfected cells can be identified by colabeling with nuclear localized tagRFPT.

(I) Quantification of Bodipy-Cyc fluorescence signal: each data point represents values from 50 to 100 transfected cells. The controls, including data from a parental plasmid (pCIT), Smo and SmoM2 expressing cells were displayed as the dashed lines. Mean (± SD) was calculated from four replicate samples. Scale bar: 10 μm.

See also Figures S2 and S4.

FA displayed a dose-dependent competition of Bodipy-Cyc binding to wild-type Smo, similar to other small molecules that directly bind Smo (SAG, and GDC0449), or that likely interact directly with Smo based on similar competition assays (SANT-1) (Figures 2H and 2I) (Chen et al., 2002a, 2002b; Frank-Kamenetsky et al., 2002; Yauch et al., 2009). In contrast, FKL induces Smo accumulation in the PC but does not compete with Bodipy-Cyc, reflecting an indirect action through its protein kinase A target (Milenkovic et al., 2009; Wilson et al., 2009). Weak pathway activation induced by FA was attenuated by Smo antagonists (Figure 2A) and depended on endogenous Smo as activation was not observed in fibroblasts lacking Smo activity (Figure S2D). SANT-1 and GDC0449 inhibit FA promoted accumulation of Smo in the PC (Figures S2E and S2F). Collectively, these data support a direct interaction between FA and Smo.

Antagonistic Drug-Drug Interactions between FA and Smo Antagonists

Considering that GCs and various Hh pathway antagonists may share a common Smo target, and GCs are widely used to suppress inflammation in conjunction with cancer therapy, we next asked whether we could observe a potential GC crosstalk with Smo antagonists in cell culture assays. Hh pathway inhibition by GDC0449, Cyc and SANT-1, as measured by both Gli-luciferase induction (Figure 3A; Figure S3) and Smo ciliary localization (Figures 3B and 3C; Figure S3), was dramatically reduced

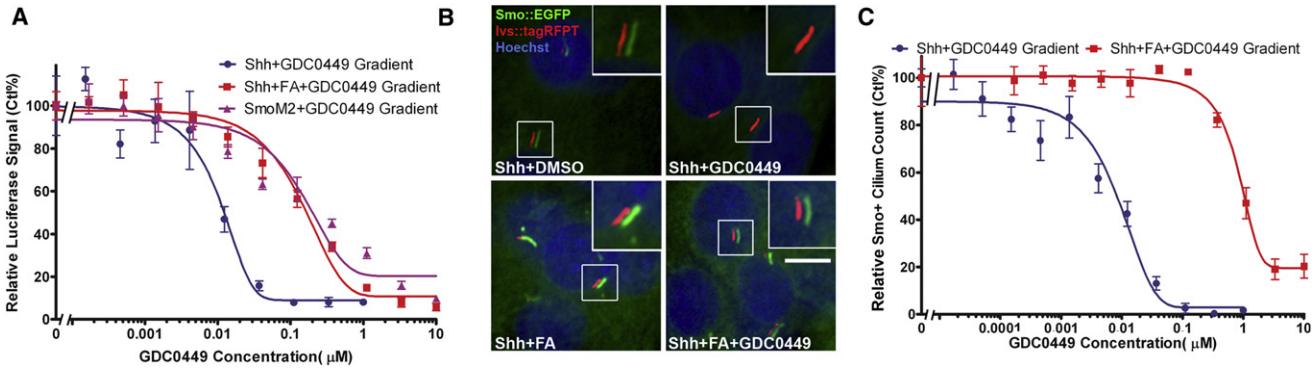

Figure 3. Drug-Drug Interaction between FA and GDC0449

(A) GDC0449 dose-dependent inhibition of Shh-stimulated Hh pathway activity in the presence or absence of 10 μM FA, or SmoM2 expressing cell lines.

(B) Representative images of Smo::EGFP/Ivs::tagRFPT cells treated with GDC0449 and Shh in the presence or absence of 10 μM FA. GDC0449 was coapplied at 111 and 1,111 nM respectively with Shh and Shh+FA.

(C) Relative Smo::EGFP+ cilium count of GDC0449's dose-dependent inhibition of Shh ligand-stimulated accumulation of ciliary Smo in the presence or absence of 10 μM FA. Measurements were performed in quadruplicate. Several hundred cells were analyzed in each sample to assess the accumulation of Smo in the PC from data in (B). Data plotted are mean (± SD). Scale bar: 5 μm.

See also Figures S3 and S4.

in vitro in the presence of FA. Thus, FA cotreatment leads to a drug-dependent alteration of cellular response to chemical inhibitors of Smo. This may occur through competition, or the requirement for a higher level of GDC-0449 to inhibit Hh-driven pathway activity in the presence of GC, but the outcome resembles the genetic resistance seen with a dominant active Smo mutation (SmoM2) (Figure 3A).

Common Properties of FA and TA in Modulating Smo Localization and Hh Pathway Activity

We next assessed whether the observations for FA were replicated by a second clinically approved GC, triamcinolone acetonide (TA). TA was slightly more potent than FA in Smo ciliary translocation assay (Figure 1B). Similar to FA, TA only evoked a Gli-mediated transcriptional response at much higher doses than those that induced Smo ciliary accumulation, although the Hh pathway was activated to higher levels than measured on FA treatment (Figure S4A). No activation was observed in $Smo^{-/-}$ embryonic fibroblast cells as expected (Figure S2D). Further, at 10 μM TA enhanced the response to Hh ligand (Figure S4B), a dose that does not sufficient to induce ligand-independent pathway activity (Figure S4A). TA also displayed a dose-dependent competition with Bodipy-Cyc for binding to Smo (Figures S4C and S4D). More importantly, 10 μM TA induced a dose-response shift for GDC0449 mediated inhibition of Hh pathway activity, and Smo ciliary accumulation induced by ligand treatment (Figures S4E–S4G). Taken together, our results indicate that these, and possibly other GCs that alter Smo localization share broadly similar biological properties but further work will be required to examine the extensive set of compounds identified in our study.

Ex Vivo Studies of FA with $Ptch1^{+/-}$ CGNPs

To further explore FA actions, we isolated cerebellar granule neuron precursors (CGNPs) from $Ptch1^{+/-}$ neonates. Proliferation of CGNP is Shh-dependent and *Ptch1* heterozygosity predisposes both mice and humans to develop CGNP-derived medulloblastoma (Schüller et al., 2008). Consistent with results on Hh pathway activation in NIH 3T3 cells, only very high doses of FA (120 μM) elevated the number of proliferative, phosphohistone H3 (pH3) positive CGNPs (Figures 4A and 4B). However, a lower dose of FA (10 μM) markedly enhanced Shh-driven CGNP proliferation (Figures 4C and 4D). Further, coadministration of FA (10 μM), with the Smo antagonist GDC0449, impaired GDC0449 inhibition of Shh-stimulated CGNP proliferation (Figures 4E and 4F).

GC Inhibitors of Smo Accumulation to the PC and of Smo Signaling

While a large number of GCs promote Smo ciliary accumulation, secondary assays of small molecules sharing the core GC scaffold identified two inhibitory GCs: budesonide (Bud) and ciclesonide (Cic) (Figures 5A–5C; Figures S5A–S5C). When compared with Smo promoting GCs, Bud and Cic are distinguished by bulky hydrophobic groups at positions 16 and 17 (Figure 1; Figure S1L; Figure 5A; Figure S5A). In contrast to FA and TA, Bud had no pathway inducing activity, nor did Bud induce a hypersensitive response to Hh ligand (Figures 2A–2F and 5D), reinforcing the association of hyperresponsiveness to Smo ciliary accumulation activity. As expected from the inhibition of Smo accumulation in the PC, Bud and Cic inhibited Shh-dependent activation of a Gli reporter (Figure 5E; Figure S5D). Further, Bud attenuated Smo ciliary accumulation and pathway activation by SAG (Figure 5E; Figures S5E and S5F), and also suppressed Cyc-induced Smo accumulation to the PC (Figures S5E and S5F). Bud treatment showed no effect on Wnt pathway activity (Figure S5G), consistent with a specific modulation of Hh signaling outside of its GC activity.

Bud Inhibit Ciliary Localization and Signaling of Drug-Resistant Mutants of Smo

SmoM2 encodes a dominant active Smo variant identified in a human cancer that is resistant to inhibition by available Smo antagonists at concentrations that completely suppressed

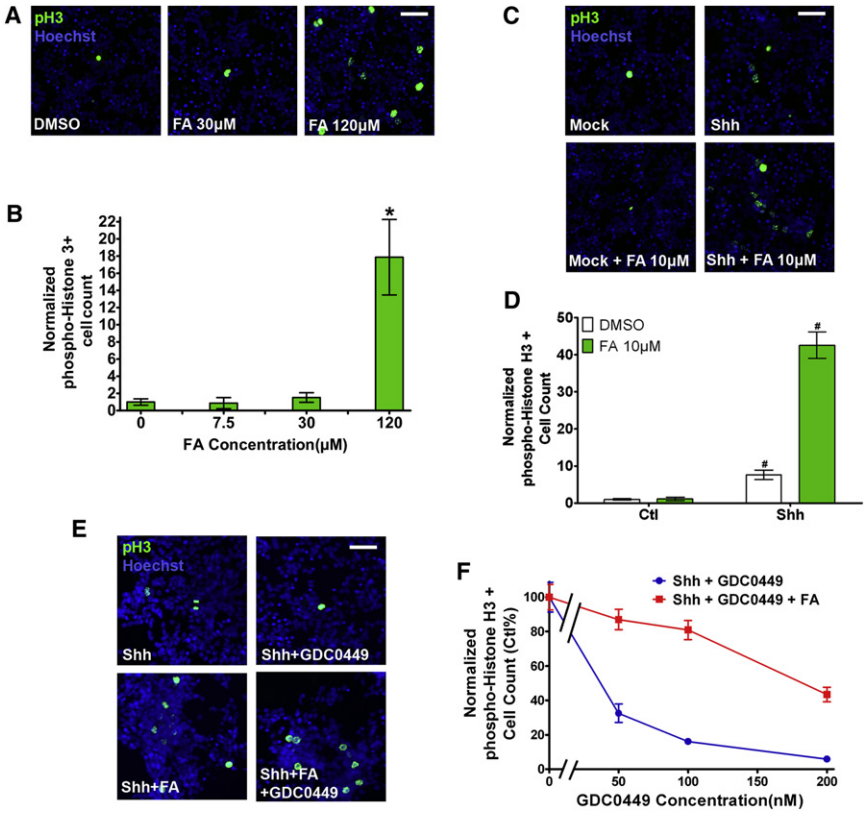

Figure 4. FA Modulates Proliferation of Cerebellar Granule Neural Precursors

CGNP proliferation was quantified based on percentage of pH3 positive cells. Representative images and measurements were shown for FA dose-dependent modulation of CGNP proliferation (A and B), promotion of Shh-stimulated CGNP proliferation by 10 μM FA (C and D), and GDC0449 dose-dependent inhibition of Shh-stimulated CGNP proliferation in the presence or absence of 10 μM FA (E and F). GDC0449 was applied at 100 nM in (E). Mean (± SD) was calculated from four replicate samples each containing over a thousand cells. *p = 0.0003(t test). #p < 0.0001 (t test). Scale bar: 20 μm.

wild-type Smo activity (Figures S5H–S5K) (Xie et al., 1998). Unexpectedly, both Bud and Cic attenuated SmoM2 ciliary localization, and downstream pathway activity, as effectively as wild-type Smo (Figures 5F–5H; Figures S5L and S5M). Bud and Cic did not disrupt ciliary structure or ciliary trafficking: acetylated-tubulin (acet-tub), Ivs::tagRFPT, and Arl13b::tagRFPT within the PC were unaltered on treatment (Figures S5N–S5R).

The emergence of a drug-resistant form of Smo with a D473H mutation was reported in a MB patient during treatment with GDC0449. The appearance of this mutation associated with a re-emergence of the tumor (Yauch et al., 2009). This finding has triggered a search for antagonists that effectively inhibit the activity of both wild-type and mutant forms of Smo (Dijkgraaf et al., 2011; Kim et al., 2010; Tao et al., 2011). We examined Bud and GDC0449 in parallel for their inhibition of Hh-induced SmoD473H activity, and the corresponding ciliary localization. $Smo^{-/-}$ MEF cells were transfected independently with wild-type and D473H mutant forms of Smo. Both forms rescued the cell's response to Hh ligand (Figure S5S). As expected, the D473H mutation conferred a dramatic resistance to GDC0449's inhibitory action on both Hh pathway activity and Smo ciliary localization (Figures S5T–S5V). In contrast, Bud showed similar efficacies in inhibiting wild-type Smo and SmoD473H activity in both assays (Figures 5I–5K).

To investigate the site of Bud action in the Hh pathway, we examined Hh signaling activity following removal of suppressor of Fused (suFU) activity, a Gli repressor functioning downstream of Smo. Distinct from GANT61 (Lauth et al., 2007), Bud failed to suppress ligand-independent Hh pathway activity induced by loss of suFU function (Figure 5L). Together these data suggest that Bud may act at the level of Smo but through a different mechanism than other Smo-interacting antagonists including SANT-1, Cyc, and GDC0449, and also distinct from FA and SAG. Consistent with a unique inhibitory action, Bud failed to compete with Bodipy-Cyc even at levels well above the inhibitory maximum (100 μM; Figures 5M and 5N). Further, whereas FA competed with GDC0449 to suppress effective pathway inhibition (Figure 3), Bud enhanced GDC0449's activity to block Smo accumulation at the PC and Hh pathway inhibition (Figure 6).

DISCUSSION

The interaction of GCs with the Hh pathway leads to several important observations. First, all small molecules that induce ligand-independent Smo accumulation to the PC characterized to date either activate or inhibit Smo activity. Agonists include SAG and purmorphamine (Chen et al., 2002b; Frank-Kamenetsky et al., 2002; Sinha and Chen, 2006). Cyc though an antagonist also induces Smo translocation to the PC (Rohatgi et al., 2009; Wang et al., 2009; Wilson et al., 2009). Several lines of evidence indicate that whereas Smo accumulation in the PC is essential for signaling, accumulation is not sufficient, with additional ligand-dependent actions being required to generate an active form of Smo (Rohatgi et al., 2009; Wang et al., 2009; Wilson et al., 2009). Together, our data suggest that many GCs can function in a novel mechanism that synergizes with Hh-ligand-directed signaling by promoting accumulation of Smo within the PC. The synergistic effect might result from bypassing a Ptch1-mediated "barrier" for Smo entry to the PC facilitating the activation of Smo, which appears to be restricted to this organelle. The mechanism of divergent pharmacological modulations of Smo ciliary translocation and its activity is not understood. A recent report suggested that Smo phosphorylation plays a role in its ciliary translocation and activation (Chen et al., 2011). Further study of small molecule directed changes in Smo phosphorylation will enhance our

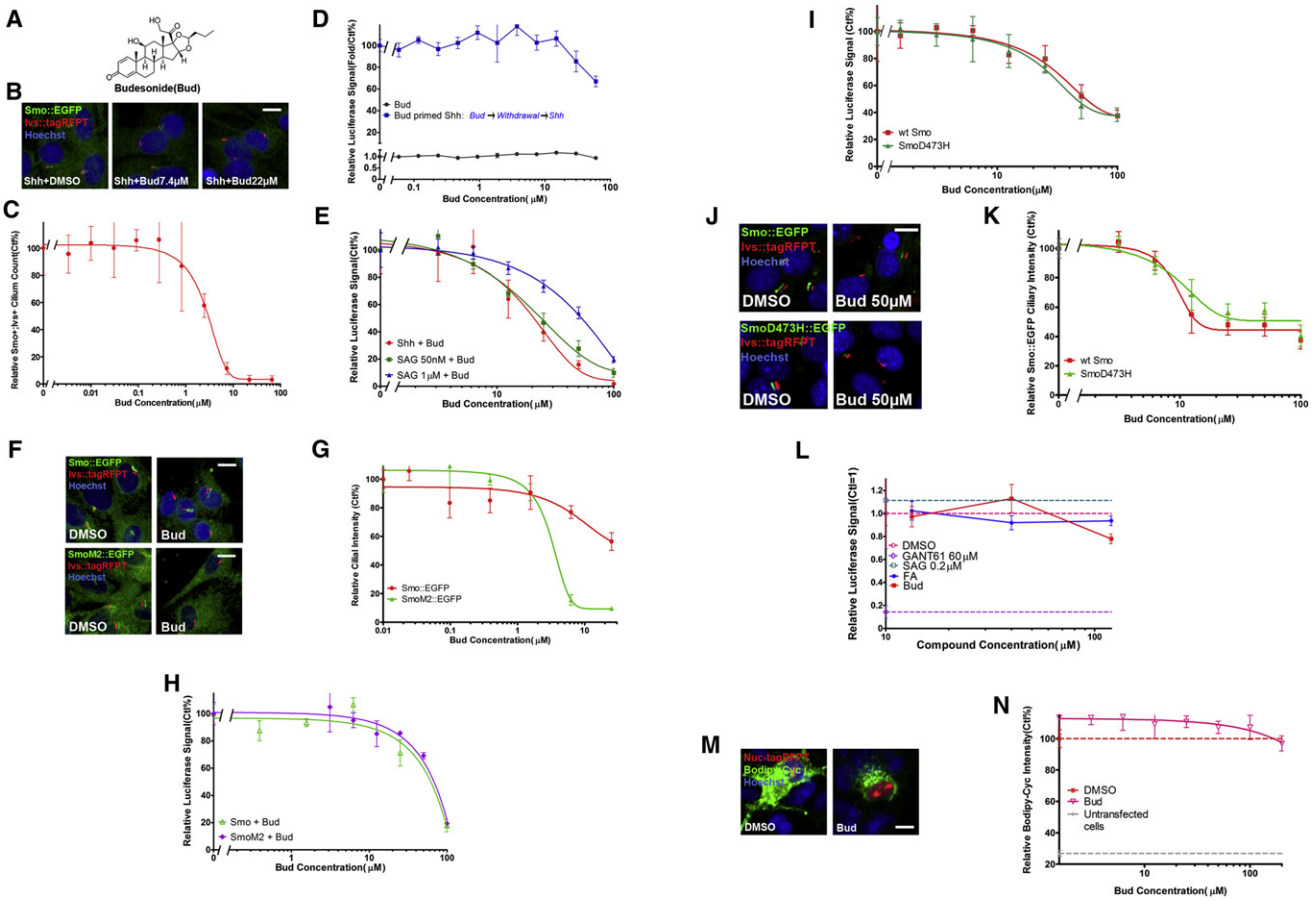

Figure 5. Bud Inhibits Hh Pathway Activity Induced by Various Stimuli and Does Not Compete with Cyc for Binding Smo

(A) The chemical structure of Bud.

(B and C) representative images (B) and quantification of Smo ciliary localization (C) in Smo::EGFP/Ivs::tagRFPT cells treated with Shh and varying concentrations of Bud.

(D) Measurement of Hh pathway activity in cells treated with Bud only or Bud followed by Shh.

(E) Dose-dependent inhibition of Hh pathway activity by Bud on Shh or SAG treatment, 50 nM or 1 μM, respectively.

(F and G) representative images (F) and quantification of Smo::EGFP or SmoM2::EGFP ciliary intensity (G) from cells treated with Bud. Bud was used at 22.2 μM in (F).

(H) Bud's dose-dependent inhibition of Hh pathway activity induced by overexpression of wild-type Smo and SmoM2 respectively.

(I) Bud's dose-dependent inhibition of Hh pathway activity induced by Shh ligand in $Smo^{-/-}$ cells transfected with constructs expressing wild-type Smo and SmoD473H, respectively.

(J and K) representative images (J) and quantification of Smo::EGFP or SmoD473H::EGFP ciliary intensity (K) from cells treated with Bud.

(L) Measurement of Hh pathway activity in $suFU^{-/-}$ cells treated with Bud and FA, respectively. DMSO and SAG were used as negative controls and GANT61 was a positive control.

(M and N) representative images (M) and quantification of Bodipy-Cyc intensity in Smo-expressing cos7 cells (N) treated with Bodipy-Cyc and Bud. Vehicle was used for comparison. Bud was used at 200 μM in (M). All quantitative data represent mean (± SD) from either quadruplicated samples (imaging assays) or triplicate experiments (Gli-luciferase assays). Quantifications of ciliary localization involved over a thousand cells per sample whereas 50–100 Smo expressing cells were analyzed in each treatment for Bodipy-Cyc competition assay. Scale bar: 5 μm.

See also Figure S5.

understanding of the significance of phosphorylation in localization and activity.

Second, the finding of a potential effect of Smo promoting GCs in modulating the Hh response highlights the value of a "direct target screen" focusing on critical parameters of target action. To date, most small molecule Hh pathway modulators have been identified through "end-point" transcriptional assays. However, because of their modest effects on transcription, GC interactions are not readily detected with this screening approach. Such disparity suggests that the mechanism of pharmacological induction of Smo accumulation to the primary cilium and its retention there is divergent from that of its activation.

Third, the dose of GC required to modify Smo localization (EC_{50}s > 1 μM) is significantly higher than that required to directly modulate GC receptor-based transcriptional responses [EC_{50}s < 10 nM or lower (Johnson, 1998)]. Thus, we believe GCs likely act directly on Smo at high concentrations, and not indirectly

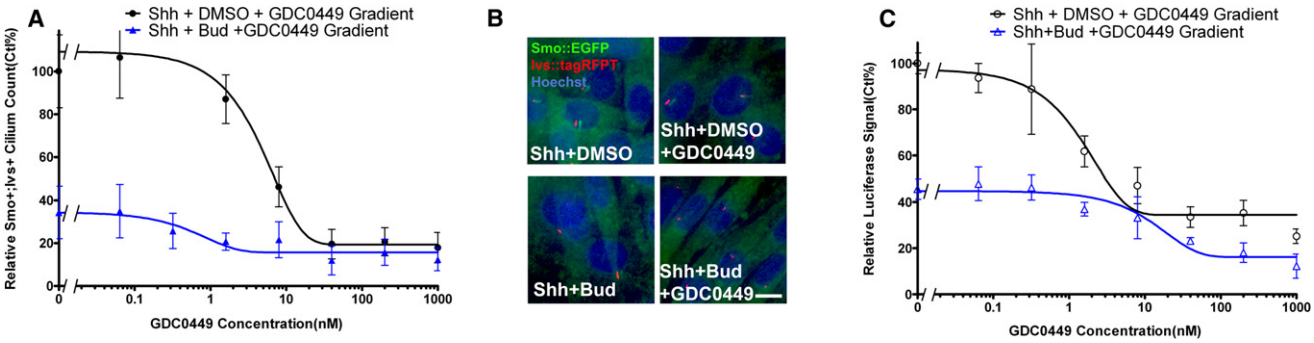

Figure 6. GDC0449 and Bud Combinatorially Inhibit Smo-Directed Hedgehog Signaling

(A and B) Quantification of Smo ciliary localization (A) and representative images (B) of Smo::EGFP/Ivs::tagRFPT cells treated with GDC0449 and Shh in the presence or absence of 10 μM Bud. In (B), GDC0449 was coapplied at 1.6 nM with Shh and Shh+Bud, respectively.

(C) GDC0449 dose-dependent inhibition of Shh-stimulated Hh pathway activity in the presence or absence of 10 μM Bud. Data plotted are mean (± SD) from four biological replicates (A) analyzing over a thousand of cells or three biological replicates (C). Scale bar: 5 μm.

through a nuclear hormone receptor triggered transcriptional regulatory action.

Fourth, naturally occurring hydrocortisone and cortisone show different potencies in accumulating Smo to the PC (Figures 1A and 1B). 11β-hydroxysteroid dehydrogenase type 2 (HSD11β2), an enzyme that transforms hydrocortisone into cortisone, is upregulated by Hh signaling in CGNPs (Heine and Rowitch, 2009), whereas HSD11β1, an enzyme that mainly catalyzes the reverse reaction, was recently discovered as a target gene for Hh signaling in prostate cancer tissue (Shaw et al., 2009). Taken together, these findings suggest potential feedback mechanisms linking the Hh transcriptional output to steroid regulation of Smo action.

Fifth, inflammation and cancer are linked, necessitating combinatorial therapies to treat both aspects of disease (Mantovani et al., 2008). To this end, GCs are frequently coadministered to patients receiving anticancer therapies. However, GCs are reported to enhance cancers of the breast (Sui et al., 2006), colon (Zhang et al., 2006a), lung (Herr et al., 2003), ovary (Sui et al., 2006; Zhang et al., 2006b), and pancreas (Zhang et al., 2006c), and to increase the metastatic potential of breast cancer (Sherlock and Hartmann, 1962). Among these are glucocorticoids that promote Smo ciliary accumulation in the current study. Further, FA is reported to act as a tumor promoter in the skin (Fukao et al., 1988). Our studies also raise the possibility of high dosing of glucocorticoids leading to off-target action of glucocorticoid agents in the Hh pathway, modifying therapeutic outcome: for example, in Hh antagonist-directed cancer therapy. Whether an effective dose for GC drug-mediated crosstalk is reached during therapeutic administration is not clear, but the pharmacokinetics of certain GC drugs in human patients may warrant further investigation. For example, a peak plasma concentration of Dexamethasone, a broadly used GC in cancer patients, has been reported at >10 μM after a single high dose (Brady et al., 1987), which falls in the range where significant Smo cilial accumulation occurs in vitro (data not shown). Long-term systematic treatment, common in cancer therapy, might result in longer exposure to higher concentrations. Further, high dose of glucocorticoids are given to preterm infants to accelerate maturation of the lungs. Whether glucocorticoids in this scenario may influence developmental Hh signaling is not known.

Sixth, our data suggest that most GCs likely share a similar interaction site with a broad range of agonists and antagonists including SAG, GDC0449, SANT-1, and Cyc, or modify Smo on binding to block access to this binding region. In contrast, Bud-like GCs do not compete with other Smo antagonists. Further, Bud works equally well inhibiting wild-type Smo and mutant forms of Smo refractory to clinically active inhibitory compounds. Thus, it may act more like an allosteric regulator of Smo activity. Interestingly, GDC0449-resistant SmoD473H can be readily inhibited by its related benzimidazole HhAntag (Dijkgraaf et al., 2011). Subsequent efforts to improve Bud potency should keep in mind the clinical imperative of pan-inhibition of Smo mutant forms. Collectively, our findings highlight the potential to develop new drugs around a GC scaffold that may synergize with compounds currently undergoing clinical development to enhance anti-Hh-based cancer therapies and may also reveal more about the ways in which Smo trafficking and activity are regulated.

SIGNIFICANCE

For some time, the hedgehog pathway has been recognized as a key regulator of embryonic development and, as such, has been implicated in a variety of birth defects. However, especially over the past decade, this pathway has been shown to participate directly or indirectly in the growth of various types of solid tumors, including basal cell carcinoma and medulloblastoma, and blood malignancies. As such, the pathway has been targeted by an ever-larger number of pharmaceutical companies, with Vismodegib, developed by Genentech and Curis, being the first hedgehog inhibitor approved by the FDA. For work described in this paper, we established an image-based screen in which we measured the translocation of the key signaling protein, Smoothened, from the cytoplasm to the primary cilium. Smoothened is the target of Vismodegib and of many of the other inhibitors being developed, and its translocation is one of the key events in propagating a hedgehog signal from the membrane to the nucleus. Interestingly, functional antagonists may either stimulate (cyclopamine) or inhibit (Vismodegib)

translocation, suggesting more complexity to Smoothened signaling than had been realized initially. We found that various types of glucocorticoids, when used at relatively high concentrations, can act as Smoothened modulators. One class, represented by fluocinolone acetonide and triamcinolone acetonide, appears to bind to Smoothened, stimulate its cilial localization and can enhance hedgehog signaling. Another chemically related class, represented by budesonide, may bind to a different site on Smoothened, inhibits Smoothened translocation and blocks hedgehog pathway activity. Budesonide has another interesting property—not shared by Vismodegib—of inhibiting different mutated forms of Smoothened, including one that has been shown to arise in patients with medulloblastoma. It appears that additional small molecule focused probing of the hedgehog pathway may provide, in the future, even more useful information and, perhaps, a few surprises.

EXPERIMENTAL PROCEDURES

Cell Culture

NIH/3T3 cells were maintained in DMEM containing 10% (v/v) calf serum, penicillin, streptomycin, and L-glutamine. HEK293, L, cos7, and suFU$^{-/-}$ mouse embryonic fibroblast cells were maintained in DMEM containing 10% (v/v) fetal bovine serum, penicillin, streptomycin, and L-glutamine. Smo::EGFP and Ivs:: tagRFPT were cloned into pBabe retroviral constructs. Smo::EGFP/Ivs::tagRFPT stable cell lines was generated through viral infecting NIH/3T3 cells according to the procedure described previously (Wang et al., 2009). A ShhLightII cell line (ATCC) was used for Gli-luciferase reporter assays. This line contains a stably integrated Gli-responsive firefly luciferase reporter and a constitutive *Renilla* luciferase expression construct (Taipale et al., 2000). A subclone of this cell line was created expressing a stably integrated SmoM2 expression construct. Shh conditioned medium was collected from cos7 cells transfected with an expression construct encoding the amino terminal 19 kDa signaling peptide of Shh and used at 13.7 (± 3.0) nM unless stated otherwise. Control conditioned medium was collected from cos7 cells transfected with an empty plasmid. Wnt3a conditioned medium was collected from an L cell line stably expressing a Wnt3a expression construct. Control-conditioned medium was collected from wild-type L cells. All conditioned medium were diluted 1:10 prior to assay.

Reagents

Chemical libraries screening utilized the Library of Pharmacologically Active Compounds (LOPAC, Sigma-Aldrich), the Spectrum Collection (Microsource Discovery Systems), and the Prestwick Chemical Library (Prestwick Chemical), along with a custom collection of additional biologically annotated chemistries absent from the above pre-plated reference collections. Glucocorticoids, cyclopamine, forskolin, mouse monoclonal antiacetylated tubulin antibody for follow-up studies were purchased from Sigma. SAG was purchased from Axxora Platform. SANT-1 was obtained from Tocris Biosciences. GDC0449 was purchased from Selleck Chemicals. BODIPY-cyclopamine was purchased from Toronto Research Chemicals. All small molecule stock solutions were prepared by dissolving in DMSO at 1 or 10 mM and stored at −20°C. Mouse recombinant ShhN purified protein (IIShhN) was a gift from Dr. Pepinsky (Biogen Inc). Rabbit polyclonal antidetyrosinated α-tubulin (Glu-tub) was from Chemicon, Mouse monoclonal anti-Arl13b antibody was from Antibody Incorporated. Secondary antibodies were from Life Technologies. Transfection was performed using Fugene6 or Fugene HD (Roche).

Imaging Assays

Cells were cultured and treated in 384-well imaging plate precoated with poly-D-Lysine (Greiner Bio-one), fixed with 4% paraformaldehyde (Electron Microscopy Sciences), and stained with Hoechst (Life Technologies). Immunofluorescence staining was conducted with standard procedures when necessary. Images were collected using Opera High Content Screening System (PerkinElmer). ActivityBase (IDBS), Pipeline Pilot (Accelrys), Excel (Microsoft), and Prism (GraphPad) were used for high content screening data management and analysis. Acapella 2.0 software (Evotec Technologies/PerkinElmer) was used to perform multiparametric image quantification. All the comparative images were scanned with identical microscopic setting and analyzed with the same input parameters.

Hh and Wnt Activity Assays

ShhLightII cells and SmoM2/LightII cells were cultured and treated in 96-well assay plates (Corning) and incubated with Duo-Glo luciferase substrates (Promega) to sequentially measure firefly and renilla luciferase activity. Smo, or GFP, expression plasmids were cotransfected into 3T3 cells together with a Gli-responsive firefly reporter and a TK-renilla luciferase reporter construct to monitor effects of Smo overexpression. Cotransfection of the two reporter constructs was conducted in assays measuring Hh pathway activity in suFU$^{-/-}$ cells. Wnt activity was measured following cotransfection of a Topflash and renilla luciferase reporter. In both Hh and Wnt activity assays, renilla luciferase reporter activity, or mass of protein, was used to normalize expression values. Luciferase signal was read by TopCount NX Microplate Scintillation and Luminescence Counter (PerkinElmer). Quantitative PCR probes for *Ptch1*, *Gli1*, and *β-actin* were purchased from Applied Biosystems. Reactions and measurements were performed using on an Applied Biosystems 7900HT at Harvard FAS Center of System Biology. *β-actin* was used to normalize *Ptch1* and *Gli1* values.

Bodipy-Cyclopamine Competition Assays

Cos7 cells were transfected with a plasmid that coexpresses Smo and a nuclear localized tagRFPT marker (pCIT-Smo). The empty parental construct (pCIT) and a construct that coexpress SmoM2 were used as controls to assess specificity and background signal. Three days after transfection, cells were incubated with 5 nM Bodipy-cyclopamine, with or without additional compounds, for 1 hr at 37°C. Cells were then fixed and stained with Hoechst. Images were collected with the Opera High Content Screen System. Fluorescence values were assessed in transfected cells (red nuclei) with a program developed by the authors using Acapella 2.0 software. All of images were scanned with identical microscopic setting and analyzed with the same input parameters.

CGNP Proliferation Assays

CGNP primary cells were isolated from P7 Ptch1$^{+/-}$ mice as previously reported (Chan et al., 2009). Cells were seeded in poly-D-lysine coated imaging plates (Greiner Bio-one), treatments were applied 2 hr thereafter and last for 36 hr. Cells then were fixed with 4% paraformaldehyde (Electron Microscopy Sciences), and stained with anti-pH3 antibody (Upstate; 1:100) followed by a secondary antibody (Invitrogen) and Hoechst (Invitrogen). Images were collected and cell proliferation quantified with a program developed by the authors utilizing Acapella 2.0 software. All of the images in each experiment were collected with identical microscopic settings and analyzed with identical input parameters.

SUPPLEMENTAL INFORMATION

Supplemental Information includes five figures and can be found with this article online at http://dx.doi.org/10.1016/j.chembiol.2012.06.012.

ACKNOWLEDGMENTS

We are very grateful to C.T. Walsh, S.L. Schreiber, and A. Saghatelian for critical review of our results and helpful discussions. We thank J.W. Lichtman, R.Y. Tsien, M.P. Scott, and P.T. Chuang for sharing reagents. We thank R.A. Segal and X. Zhao for technical assistance on CGNP cell culture and our colleagues in the McMahon and Rubin laboratories for support on our research. We also thank Dr. James A. Thomson for his support. This work was funded by the Harvard Stem Cell Institute (DP-0033-08-02 to A.P.M. and L.L.R.) and the National Institutes of Health (R37 NS033642 to A.P.M.). Y.W., L.L.R., and A.P.M. hold patent positions around Hedgehog signaling and drug discovery platforms. Intellectual property protection is being

developed about the assay and compounds herein. Y.W., L.L.R., and A.P.M. conceived the project. Y.W. developed and validated the assay. Primary screens and secondary assays and data analysis were performed by Y.W., J.B., L.D., A.C.A., K.L., J.W.Y., J.M.Y.N., and T.C.; Y.W., L.L.R., and A.P.M. wrote the paper.

Received: August 10, 2011
Revised: May 24, 2012
Accepted: June 11, 2012
Published: August 23, 2012

REFERENCES

Allison, M. (2012). Hedgehog hopes lifted by approval... and stung by failure. Nat. Biotechnol. *30*, 203.

Besschetnova, T.Y., Kolpakova-Hart, E., Guan, Y., Zhou, J., Olsen, B.R., and Shah, J.V. (2010). Identification of signaling pathways regulating primary cilium length and flow-mediated adaptation. Curr. Biol. *20*, 182–187.

Brady, M.E., Sartiano, G.P., Rosenblum, S.L., Zaglama, N.E., and Bauguess, C.T. (1987). The pharmacokinetics of single high doses of dexamethasone in cancer patients. Eur. J. Clin. Pharmacol. *32*, 593–596.

Buonamici, S., Williams, J., Morrissey, M., Wang, A., Guo, R., Vattay, A., Hsiao, K., Yuan, J., Green, J., Ospina, B., et al. (2010). Interfering with resistance to smoothened antagonists by inhibition of the PI3K pathway in medulloblastoma. Sci. Transl. Med. *2*, 51ra70.

Caspary, T., Larkins, C.E., and Anderson, K.V. (2007). The graded response to Sonic Hedgehog depends on cilia architecture. Dev. Cell *12*, 767–778.

Chan, J.A., Balasubramanian, S., Witt, R.M., Nazemi, K.J., Choi, Y., Pazyra-Murphy, M.F., Walsh, C.O., Thompson, M., and Segal, R.A. (2009). Proteoglycan interactions with Sonic Hedgehog specify mitogenic responses. Nat. Neurosci. *12*, 409–417.

Chen, J.K., Taipale, J., Cooper, M.K., and Beachy, P.A. (2002a). Inhibition of Hedgehog signaling by direct binding of cyclopamine to Smoothened. Genes Dev. *16*, 2743–2748.

Chen, J.K., Taipale, J., Young, K.E., Maiti, T., and Beachy, P.A. (2002b). Small molecule modulation of Smoothened activity. Proc. Natl. Acad. Sci. USA *99*, 14071–14076.

Chen, Y., Sasai, N., Ma, G., Yue, T., Jia, J., Briscoe, J., and Jiang, J. (2011). Sonic Hedgehog dependent phosphorylation by CK1α and GRK2 is required for ciliary accumulation and activation of smoothened. PLoS Biol. *9*, e1001083.

Dijkgraaf, G.J., Alicke, B., Weinmann, L., Januario, T., West, K., Modrusan, Z., Burdick, D., Goldsmith, R., Robarge, K., Sutherlin, D., et al. (2011). Small molecule inhibition of GDC-0449 refractory smoothened mutants and downstream mechanisms of drug resistance. Cancer Res. *71*, 435–444.

Frank-Kamenetsky, M., Zhang, X.M., Bottega, S., Guicherit, O., Wichterle, H., Dudek, H., Bumcrot, D., Wang, F.Y., Jones, S., Shulok, J., et al. (2002). Small-molecule modulators of Hedgehog signaling: identification and characterization of Smoothened agonists and antagonists. J. Biol. *1*, 10.

Fukao, K., Tanimoto, Y., Kayata, Y., Yoshiga, K., Takada, K., and Okuda, K. (1988). Effects of fluocinolone acetonide on mouse skin sterol metabolism and two-stage carcinogenesis. Carcinogenesis *9*, 1661–1664.

Goetz, S.C., and Anderson, K.V. (2010). The primary cilium: a signalling centre during vertebrate development. Nat. Rev. Genet. *11*, 331–344.

Hambardzumyan, D., Becher, O.J., Rosenblum, M.K., Pandolfi, P.P., Manova-Todorova, K., and Holland, E.C. (2008). PI3K pathway regulates survival of cancer stem cells residing in the perivascular niche following radiation in medulloblastoma in vivo. Genes Dev. *22*, 436–448.

Han, Y.G., Kim, H.J., Dlugosz, A.A., Ellison, D.W., Gilbertson, R.J., and Alvarez-Buylla, A. (2009). Dual and opposing roles of primary cilia in medulloblastoma development. Nat. Med. *15*, 1062–1065.

Heine, V.M., and Rowitch, D.H. (2009). Hedgehog signaling has a protective effect in glucocorticoid-induced mouse neonatal brain injury through an 11betaHSD2-dependent mechanism. J. Clin. Invest. *119*, 267–277.

Herr, I., Ucur, E., Herzer, K., Okouoyo, S., Ridder, R., Krammer, P.H., von Knebel Doeberitz, M., and Debatin, K.M. (2003). Glucocorticoid cotreatment induces apoptosis resistance toward cancer therapy in carcinomas. Cancer Res. *63*, 3112–3120.

Johnson, M. (1998). Development of fluticasone propionate and comparison with other inhaled corticosteroids. J. Allergy Clin. Immunol. *101*, S434–S439.

Kim, J., Kato, M., and Beachy, P.A. (2009). Gli2 trafficking links Hedgehog-dependent activation of Smoothened in the primary cilium to transcriptional activation in the nucleus. Proc. Natl. Acad. Sci. USA *106*, 21666–21671.

Kim, J., Lee, J.J., Kim, J., Gardner, D., and Beachy, P.A. (2010). Arsenic antagonizes the Hedgehog pathway by preventing ciliary accumulation and reducing stability of the Gli2 transcriptional effector. Proc. Natl. Acad. Sci. USA *107*, 13432–13437.

Lauth, M., Bergström, A., Shimokawa, T., and Toftgård, R. (2007). Inhibition of GLI-mediated transcription and tumor cell growth by small-molecule antagonists. Proc. Natl. Acad. Sci. USA *104*, 8455–8460.

Mantovani, A., Allavena, P., Sica, A., and Balkwill, F. (2008). Cancer-related inflammation. Nature *454*, 436–444.

Milenkovic, L., Scott, M.P., and Rohatgi, R. (2009). Lateral transport of Smoothened from the plasma membrane to the membrane of the cilium. J. Cell Biol. *187*, 365–374.

Riobó, N.A., Lu, K., Ai, X.B., Haines, G.M., and Emerson, C.P., Jr. (2006). Phosphoinositide 3-kinase and Akt are essential for Sonic Hedgehog signaling. Proc. Natl. Acad. Sci. USA *103*, 4505–4510.

Rohatgi, R., Milenkovic, L., and Scott, M.P. (2007). Patched1 regulates hedgehog signaling at the primary cilium. Science *317*, 372–376.

Rohatgi, R., Milenkovic, L., Corcoran, R.B., and Scott, M.P. (2009). Hedgehog signal transduction by Smoothened: pharmacologic evidence for a 2-step activation process. Proc. Natl. Acad. Sci. USA *106*, 3196–3201.

Rubin, L.L., and de Sauvage, F.J. (2006). Targeting the Hedgehog pathway in cancer. Nat. Rev. Drug Discov. *5*, 1026–1033.

Schrøder, J.M., Schneider, L., Christensen, S.T., and Pedersen, L.B. (2007). EB1 is required for primary cilia assembly in fibroblasts. Curr. Biol. *17*, 1134–1139.

Schüller, U., Heine, V.M., Mao, J., Kho, A.T., Dillon, A.K., Han, Y.G., Huillard, E., Sun, T., Ligon, A.H., Qian, Y., et al. (2008). Acquisition of granule neuron precursor identity is a critical determinant of progenitor cell competence to form Shh-induced medulloblastoma. Cancer Cell *14*, 123–134.

Shaw, A., Gipp, J., and Bushman, W. (2009). The Sonic Hedgehog pathway stimulates prostate tumor growth by paracrine signaling and recapitulates embryonic gene expression in tumor myofibroblasts. Oncogene *28*, 4480–4490.

Sherlock, P., and Hartmann, W.H. (1962). Adrenal steroids and the pattern of metastases of breast cancer. JAMA *181*, 313–317.

Sinha, S., and Chen, J.K. (2006). Purmorphamine activates the Hedgehog pathway by targeting Smoothened. Nat. Chem. Biol. *2*, 29–30.

Sommer, P., and Ray, D.W. (2008). Novel therapeutic agents targeting the glucocorticoid receptor for inflammation and cancer. Curr. Opin. Investig. Drugs *9*, 1070–1077.

Sui, M.H., Chen, F., Chen, Z., and Fan, W.M. (2006). Glucocorticoids interfere with therapeutic efficacy of paclitaxel against human breast and ovarian xenograft tumors. Int. J. Cancer *119*, 712–717.

Taipale, J., Chen, J.K., Cooper, M.K., Wang, B., Mann, R.K., Milenkovic, L., Scott, M.P., and Beachy, P.A. (2000). Effects of oncogenic mutations in Smoothened and Patched can be reversed by cyclopamine. Nature *406*, 1005–1009.

Tao, H., Jin, Q., Koo, D.I., Liao, X., Englund, N.P., Wang, Y., Ramamurthy, A., Schultz, P.G., Dorsch, M., Kelleher, J., and Wu, X. (2011). Small molecule antagonists in distinct binding modes inhibit drug-resistant mutant of smoothened. Chem. Biol. *18*, 432–437.

Tremblay, M.R., McGovern, K., Read, M.A., and Castro, A.C. (2010). New developments in the discovery of small molecule Hedgehog pathway antagonists. Curr. Opin. Chem. Biol. *14*, 428–435.

Vlahos, C.J., Matter, W.F., and Brown, R.F. (1994). A Specific Inhibitor of Phosphatidylinositol 3-Kinase. J. Cell. Biochem. *269*, 5241–5248.

Wang, J., Lu, J., Bond, M.C., Chen, M., Ren, X.R., Lyerly, H.K., Barak, L.S., and Chen, W. (2010). Identification of select glucocorticoids as Smoothened agonists: potential utility for regenerative medicine. Proc. Natl. Acad. Sci. USA *107*, 9323–9328.

Wang, Y., Zhou, Z., Walsh, C.T., and McMahon, A.P. (2009). Selective translocation of intracellular Smoothened to the primary cilium in response to Hedgehog pathway modulation. Proc. Natl. Acad. Sci. USA *106*, 2623–2628.

Wang, Y., Arvanites, A.C., Davidow, L., Blanchard, J., Lam, K., Yoo, J.W., Coy, S., Rubin, L.L., and McMahon, A.P. (2012). Selective identification of Hedgehog pathway antagonists by direct analysis of smoothened ciliary translocation. ACS Chem. Biol. *7*, 1040–1048.

Watanabe, D., Saijoh, Y., Nonaka, S., Sasaki, G., Ikawa, Y., Yokoyama, T., and Hamada, H. (2003). The left-right determinant Inversin is a component of node monocilia and other 9+0 cilia. Development *130*, 1725–1734.

Wilson, C.W., Chen, M.-H., and Chuang, P.-T. (2009). Smoothened adopts multiple active and inactive conformations capable of trafficking to the primary cilium. PLoS ONE *4*, e5182.

Wong, S.Y., Seol, A.D., So, P.L., Ermilov, A.N., Bichakjian, C.K., Epstein, E.H., Jr., Dlugosz, A.A., and Reiter, J.F. (2009). Primary cilia can both mediate and suppress Hedgehog pathway-dependent tumorigenesis. Nat. Med. *15*, 1055–1061.

Xie, J., Murone, M., Luoh, S.M., Ryan, A., Gu, Q., Zhang, C., Bonifas, J.M., Lam, C.W., Hynes, M., Goddard, A., et al. (1998). Activating Smoothened mutations in sporadic basal-cell carcinoma. Nature *391*, 90–92.

Yauch, R.L., Gould, S.E., Scales, S.J., Tang, T., Tian, H., Ahn, C.P., Marshall, D., Fu, L., Januario, T., Kallop, D., et al. (2008). A paracrine requirement for hedgehog signalling in cancer. Nature *455*, 406–410.

Yauch, R.L., Dijkgraaf, G.J., Alicke, B., Januario, T., Ahn, C.P., Holcomb, T., Pujara, K., Stinson, J., Callahan, C.A., Tang, T., et al. (2009). Smoothened mutation confers resistance to a Hedgehog pathway inhibitor in medulloblastoma. Science *326*, 572–574.

Zhang, C., Kolb, A., Mattern, J., Gassler, N., Wenger, T., Herzer, K., Debatin, K.M., Büchler, M., Friess, H., Rittgen, W., et al. (2006a). Dexamethasone desensitizes hepatocellular and colorectal tumours toward cytotoxic therapy. Cancer Lett. *242*, 104–111.

Zhang, C.W., Marmé, A., Wenger, T., Gutwein, P., Edler, L., Rittgen, W., Debatin, K.M., Altevogt, P., Mattern, J., and Herr, I. (2006b). Glucocorticoid-mediated inhibition of chemotherapy in ovarian carcinomas. Int. J. Oncol. *28*, 551–558.

Zhang, C.W., Kolb, A., Büchler, P., Cato, A.C.B., Mattern, J., Rittgen, W., Edler, L., Debatin, K.M., Büchler, M.W., Friess, H., and Herr, I. (2006c). Corticosteroid co-treatment induces resistance to chemotherapy in surgical resections, xenografts and established cell lines of pancreatic cancer. BMC Cancer *6*, 61.

Zhang, J.H., Chung, T.D.Y., and Oldenburg, K.R. (1999). A simple statistical parameter for use in evaluation and validation of high throughput screening assays. J. Biomol. Screen. *4*, 67–73.

Zhang, X.M., Ramalho-Santos, M., and McMahon, A.P. (2001). Smoothened mutants reveal redundant roles for Shh and Ihh signaling including regulation of L/R symmetry by the mouse node. Cell *106*, 781–792.

